Positive Damping Region: A Graphic Tool for Passivization Analysis with Passivity Index

Xiaoyu Peng, Xi Ru, Zhongze Li, Jianxin Zhang, Xinghua Chen, Feng Liu

***Abstract*—This paper presents a geometric framework for analyzing output-feedback and input-feedforward passivization of linear time-invariant systems. We reveal that a system is passivizable with a given passivity index when the Nyquist plot for SISO systems or the Rayleigh quotient of the transfer function for MIMO systems lies within a specific, index-dependent region in the complex plane, termed the positive damping region. The criteria enable a convenient graphic tool for analyzing the passivization, the associated frequency bands, the maximum achievable passivity index, and the waterbed effect between them. Additionally, the tool can be encoded into classical tools such as the Nyquist plot, the Nichols plot, and the generalized KYP lemma to aid control design. Finally, we demonstrate its application in passivity-based power system stability analysis and discuss its implications for electrical engineers regarding device controller design trade-offs.**

***Index Terms*—passivity index, output-feedback passivization, geometric interpretation, bandwidth contraction**

I. Introduction

Passivity theory is a cornerstone concept in the stability analysis of dynamical systems [1]. Benefiting from its modularity, passivity is highly valuable for distributed analysis of practical systems [2]. With theoretical advancements, it has been extended for better descriptions of non-passive systems by incorporating output-feedback (OF) and input-feedforward (IF) structures [3]. Introducing passivity indices into the OF or IF paths enables quantification of the system's distance from passivity and the contribution to the closed-loop stability.

A core condition of passivity is the positive damping property, which usually implies positive contributions to the stability of physical systems, and a larger passivity index indicates stronger damping. For instance, the passivity index is positively correlated with the equivalent admittance in power electronic circuits, which indicates better oscillation suppression capabilities [4]. At the same time, it is desirable to broaden the passive bandwidth as wide as possible, even if the system cannot be passive for all frequencies. The situations of non-passivity throughout the whole frequency bands usually happen in practical power systems, such as the high-frequency bands of synchronous generators and power electronic devices [5]. Nevertheless, the pursuit of an expanded passive frequency bandwidth and an increased passivity index presents inherent contradictions. An excessively large passivity index results in narrower or the vanishing of passive bandwidths. Conversely, a small passivity index achieves a broader passive frequency band but does not adequately represent the system's actual damping capability.

Literature typically focuses on finding the maximum passivity index subject to passivity. For linear time-invariant (LTI) systems, mainstream transforms passivity constraints into a set of linear matrix inequalities (LMIs) via the Kalman-Yakubovich-Popov (KYP) lemma [3]. For instance, the passivization problem for systems subject to frequency-dependent quadratic constraints can be reformulated as LMIs [6]. These methods are further incorporated into extended definitions of passivity, such as differential passivity [2], and the nonlinear systems [7]. The above methods are derived from the time domain and thus implicitly require the system to satisfy passivity across the entire frequency spectrum. However, it might not be achievable via IF or OF structures [8], which can render these methods infeasible. For these systems, however, their passive frequency bands remain a concern in practice. For example, a significant topic in power electronics is designing passivization controllers within targeted frequency bands to suppress oscillations [4]. The pioneering work [9] addresses this challenge by extending the KYP lemma to a restricted frequency band, thereby relaxing the frequency-spectrum constraints. Nonetheless, akin to prior research, these LMI-based approaches hinder the exploration of the geometric interpretations of the intrinsic trade-off between the passivity index and the passive bandwidth.

Unlike existing methods, we visualize the passivization conditions on complex planes. This idea is primarily inspired by the circle criteria [3] and the disk margin theory [10], but focusing on passivization rather than stability or robustness. The contribution of this paper: we introduce positive damping (PD) conditions to determine if an LTI system can be passivized for a specific passivity index. The PD conditions are transformed into a parameter region in the complex plane. LTI systems are passivized if the transfer function's Nyquist plot for SISO systems or the Rayleigh quotient for MIMO systems falls within these regions. This geometric visualization provides a graphic tool for verifying several critical attributes: the feasibility of IF or OF passivization, the specific passivizable frequency bands, the maximum achievable passivity index and their trade-off. Moreover, this tool can facilitate passivity-based stability analysis and control design thanks

This research is supported by the Smart Grid National Science and Technology Major Project under Grant 2024ZD0801200. (*Corresponding author: Feng Liu*).

Xiaoyu Peng, Xi Ru, Zhongze Li, and Feng Liu are with Department of Electrical Engineering, Tsinghua University, Beijing, China (email: pengxy19@tsinghua.org.cn; lizz24@mails.tsinghua.edu.cn; thu.ruxi@gmail.com; lfeng@tsinghua.edu.cn).

Jianxin Zhang is with Power Dispatch Control Center, China Southern Power Grid Corporation (email: zhangjianxin@csg.cn).

Xinghua Chen is with Power Dispatch Control Center, Guangdong Power Grid Corporation (email: 1351278605@qq.com).

to the simplicity of the proposed criteria. We also show that the proposed method can be extended to generalized passivity definitions, including negative imaginariness [11].

Notation: The sets of real and complex numbers are denoted by $\mathbb{R}$ and $\mathbb{C}$. $\Re(c)$ and $\Im(c)$ represent the real and imaginary parts of a complex number $c \in \mathbb{C}$. The Rayleigh quotient of a complex matrix M is denoted as $\rho_M(x) = x^H Mx/(x^H x)$ for $x^H x \neq 0$. The normal transpose and Hermite transpose are M^T and M^H. For a real symmetric matrix M, $\lambda_{\min}(M)$ denotes its minimum eigenvalue and $M \succ 0$ for its positive definiteness. A closed disk centering on $c \in \mathbb{C}$ with a positive radius $r \in \mathbb{R}$ is denoted by $\mathcal{D}(c,r) = \{z \in \mathbb{C} : |z-c| \leq r\}$ and its boundary circle by $\partial\mathcal{D}(c,r)$. The positive damping region and frequency bands w.r.t. a passivity index σ defined in this paper are denoted by $\mathcal{P}_{\mathrm{PD}}(\sigma)$ and $\Omega_{\mathrm{PD}}(\sigma)$.

II. Preliminaries

Definition 1 (Passivity [3])**.** *Consider an LTI system with a minimal realization $\dot{x} = Ax+Bu, y = Cx+Du$. It is passive if its transfer function $H(s) = C(sI-A)^{-1}B + D$ satisfies the following conditions:*

1) *Poles of all elements of $H(s)$ are in the closed left-half plane.*
2) *For all real ω for which $j\omega$ is not a pole of any element of $H(s)$, the matrix satisfies:*

$$H(j\omega) + H^H(j\omega) \succeq 0 \tag{1}$$

3) *Any pure imaginary pole $j\omega$ of any element of $H(s)$ is a simple pole and the residue satisfies $\lim_{s\to j\omega}(s-j\omega)H(s) \succeq 0$.*

Besides, if $H(s-\varepsilon)$ is passive for a constant $\varepsilon > 0$, it is called strictly passive.

Among all three conditions in Definition 1, the second one is of most significance. For SISO systems, it reduces to $H(j\omega)+H^H(j\omega) = 2\Re(H(j\omega)) \geq 0$, i.e., the real part of its Nyquist plot stays positive, which usually implies positive damping in practice. For example, consider a power system model $H(s) = 1/(ls+r)$, where l and r denote the equivalent inductance and resistance, respectively. Then, the condition (1)$= 2r/[(l\omega)^2 + r^2]$ holds iff the circuit has resistance $r > 0$. To emphasize its significance, this paper specifically denotes it as the *positive damping (PD)* condition.

Definition 2 (Positive Damping Condition)**.** *Let $H(s)$ be a transfer matrix satisfying the domain requirements of Definition 1. We say H satisfies the PD condition at $\omega \in \mathbb{R}$ if $j\omega$ is not a pole of H and satisfies (1).*

To broaden its applicability to feedback systems with non-passive subsystems in Fig. 1(a), we often consider its equivalent system in Fig. 1(b). Then, if the OF system $\tilde{G}_1$ and the IF system $\tilde{G}_2$ are both passive, and the condition $\sigma_1+\sigma_2 \succeq 0$ is satisfied, the closed-loop system is passive [3, Chapter 6]. Note that the original subsystems in Fig. 1(a) correspond to the special case where $\sigma_1 = \sigma_2 = 0$. The formal definitions of IF and OF passivizations are given as follows:

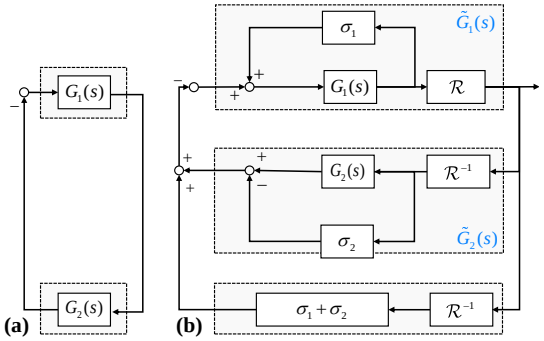

Fig. 1. Feedback interconnected system model. (a): original model. (b): equivalent model with IF passivization and OF passivization, where $\mathcal{R} = I$ for classical passivity definition. The operator is for compatibility with the latter discussions of generalized passivity definitions.

Definition 3 (Input-Feedforward Passivization)**.** *A $p \times p$ LTI system $G(s)$ is IF passivizable w.r.t. a symmetric matrix $\sigma \in \mathbb{R}^{p\times p}$ if $H(s)$ in (2) is well-defined and passive:*

$$H(s) = G(s) - \sigma \tag{2}$$

The matrix σ is called its IF passivity index.

Definition 4 (Output-Feedback Passivization)**.** *A $p \times p$ LTI system $G(s)$ is OF passivizable w.r.t. a symmetric matrix $\sigma \in \mathbb{R}^{p\times p}$ if $H(s)$ in (3) is well-defined ($I - G(s)\sigma$ invertible at all points required by Definition 1) and H is passive:*

$$H(s) = (I - G(s)\sigma)^{-1}G(s) \tag{3}$$

The matrix σ is called its OF passivity index.

The case of IF passivization is relatively simple by noticing the linear correlation between H and G. Therefore, this paper is dedicated to investigating the OF passivization and its extension to IF passivization is trivial.

III. Visualizing Passivization of MIMO Systems

A. Positive Damping Condition

Throughout the paper, we consider the transfer functions satisfying the following condition:

Assumption 1. *A transfer function is real and strictly proper.*

Theorem 1 (MIMO PD Condition)**.** *Let $G(s)$ be a transfer function matrix satisfying Assumption 1. Consider a passivity index σ and a frequency $\omega \in \mathbb{R}$ such that $j\omega$ is not a pole of G and $I - G(j\omega)\sigma$ is non-singular.*

1) *The PD condition (1) holds at the frequency ω iff:*

$$G(j\omega) + G^H(j\omega) \succeq 2G(j\omega)\sigma G^H(j\omega) \tag{4}$$

2) *A necessary condition of the PD condition (1) at the frequency ω is that the Rayleigh quotient $\rho_{G(j\omega)}(x)$ satisfies:*

$$\Re(\rho_{G(j\omega)}(x)) \geq \lambda_{\min}(\sigma)|\rho_{G(j\omega)}(x)|^2, \forall x : x^H x \neq 0 \tag{5}$$

Proof. Substituting $H = (I - G\sigma)^{-1}G$ into the PD condition (1) yields $(I - G\sigma)^{-1}G + G^H(I - \sigma G^H)^{-1} \succeq 0$. Noticing

that the complex congruent transformation with a non-singular matrix does not change the positive-definiteness, left multiplying $(I - G\sigma)$ and right multiplying $(I - G\sigma)^H = (I - \sigma G^H)$ lead to (4).

For any $x \in \mathbb{C}^p : x^H x \neq 0$, consider the quadratic form $x^H(G + G^H - 2G\sigma G^H)x \geq 0$, which can be rewritten as:

$$2\Re(x^H G x) \geq 2x^H G\sigma G^H x \tag{6}$$

Define the Rayleigh quotient $\rho_G(x) = x^H Gx/(x^H x)$. Then, the left-hand side can be transformed into $\Re(x^H Gx) = \Re(\rho_G(x)) \cdot (x^H x)$.

Then, we consider the right-hand side. Let $y = G^H x$, then $x^H G\sigma G^H x = y^H \sigma y$. Since σ is a symmetric matrix, we have:

$$y^H \sigma y \geq \lambda_{\min}(\sigma)\|y\|^2 = \lambda_{\min}(\sigma)(x^H GG^H x) \tag{7}$$

Moreover, the Cauchy-Schwarz inequality suggests:

$$\left|x^H Gx\right|^2 = \left|(G^H x)^H x\right|^2 \leq [(G^H x)^H (G^H x)] \cdot (x^H x) \tag{8}$$

which can be simplified to $x^H GG^H x \geq |x^H Gx|^2/(x^H x) = |\rho_G|^2 \cdot (x^H x)$. Combining it with (7) gives:

$$y^H \sigma y \geq \lambda_{\min}(\sigma)|\rho_G(x)|^2 \cdot (x^H x) \tag{9}$$

Substituting it into (6) yields $2\Re(\rho_G(x)) \cdot (x^H x) \geq 2\lambda_{\min}(\sigma)|\rho_G(x)|^2 \cdot (x^H x)$. Simplifying this inequality yields $\Re(\rho_G(x)) \geq \lambda_{\min}(\sigma)|\rho_G(x)|^2$. This condition must hold for $\forall x \in \mathbb{C}^p : x^H x \neq 0$, which completes the proof. □

Remark 1 (Relation with Matrix Pencil and Numerical Range)**.** *The first part of Theorem 1 has an equivalent expression: $G(s)$ meets the PD condition at ω iff $\lambda_{g,\min} \geq 1/2$, where $\lambda_{g,\min}$ is the generalized eigenvalue of $G(j\omega)+G^H(j\omega)$ and $G(j\omega)\sigma G^H(j\omega)$. The result can be directly derived from (4). Note that this is a necessary and sufficient condition. Additionally, numerical verification is straightforward, as most commercial software includes a matrix pencil function.*

The second part of Theorem 1 builds upon the Rayleigh quotient. The associated concept, numerical range, has significant applications in the study of passivity and the small-phase theorem of MIMO systems [12].

Theorem 1 implies that there exists an LMI-based convex formulation of the PD condition as follows.

Corollary 1 (LMI-based MIMO PD Condition)**.** *Let $G(s)$ be a transfer function matrix satisfying Assumption 1. Consider a passivity index $\sigma \succ 0$ and a frequency $\omega \in \mathbb{R}$ such that $j\omega$ is not a pole of G and $I - G(j\omega)\sigma$ is non-singular. Then, the PD condition (1) is satisfied iff:*

$$\begin{bmatrix} G + G^H & G \\ G^H & (2\sigma)^{-1} \end{bmatrix} \succeq 0 \tag{10}$$

Proof. By the Schur's complement lemma, (10) holds iff $\sigma^{-1} \succ 0$ and $(G + G^H) - G(\sigma^{-1}/2)^{-1}G^H = G + G^H - 2G\sigma G^H \succeq 0$, which is identical to (4). □

B. Visualization of PD Region and Its Property

The first result of Theorem 1 is sufficient and necessary but not geometrically intuitive. Alternatively, the second result can be visualized as follows. Since the Rayleigh quotient is complex, the region satisfying the condition (5) in cases $\sigma \succ 0$ can be rewritten as $\{\rho_G : \rho_G(x) \in \mathcal{P}_{\mathrm{PD}}(\sigma), \forall x^H x \neq 0\}$, where:

$$\mathcal{P}_{\mathrm{PD}}(\sigma) = \mathcal{D}\left(\frac{1}{2\lambda_{\min}(\sigma)} + j0, \frac{1}{2\lambda_{\min}(\sigma)}\right) \tag{11}$$

$\mathcal{P}_{\mathrm{PD}}(\sigma)$ is called the *output-feedback positive damping region (OF PD region)*. It describes a disk in the complex plane centered at $(1/(2\lambda_{\min}(\sigma)), j0)$ with radius $1/(2\lambda_{\min}(\sigma))$. All Rayleigh quotients $\rho_G(x)$ must lie within this disk to guarantee the PD condition. Moreover, the Toeplitz–Hausdorff theorem guarantees that the shape of $\rho_G(x)$ for a given frequency is convex. Moreover, the PD region for $\lambda_{\min}(\sigma) < 0$ is the complement of a disk, i.e., $[\mathbb{C}\backslash\mathcal{D}(1/(2\lambda_{\min}(\sigma)), 1/(2\lambda_{\min}(\sigma)))] \cup \partial\mathcal{D}(1/(2\lambda_{\min}(\sigma)), 1/(2\lambda_{\min}(\sigma)))$.

Then, the frequency bands that fulfill the PD condition, referred to as the *PD frequency band*, can be estimated from this interpretation. Furthermore, it provides a geometric explanation of why increasing the OF passivity index results in a narrower PD bandwidth and a more stringent passivity condition, as summarized by the subsequent corollary.

Definition 5 (OF PD Frequency Band)**.** *Consider a transfer function matrix $G(s)$ satisfying Assumption 1 and its OF system $H(s)$ (3) w.r.t. a passivity index σ. Then, its output-feedback positive damping frequency band (OF PD frequency band) w.r.t. σ is defined as:*

$$\begin{aligned}\Omega_{\mathrm{PD}}(\sigma) = \{\omega \geq 0 : &H(j\omega) + H^H(j\omega) \succeq 0, \\ &G(j\omega) \text{ and } I - \sigma G(j\omega) \text{ well-defined}\}\end{aligned} \tag{12}$$

Besides, define the estimated OF PD frequency bands as $\tilde{\Omega}_{\mathrm{PD}}(\sigma) = \{\omega \geq 0 : (5) \text{ is satisfied}\}$.

Corollary 2 (OF PD Bandwidth Contraction)**.** *Consider a transfer function matrix $G(s)$ satisfying Assumption 1. Then, $\Omega_{\mathrm{PD}}(\sigma) \subseteq \tilde{\Omega}_{\mathrm{PD}}(\sigma)$ holds for any passivity index $\sigma \neq 0$. Moreover, increasing σ contracts the PD frequency band, i.e.:*

1) *For any indices σ_1 and σ_2 satisfying $\sigma_2 \succ \sigma_1 \succ 0$, it holds that $\tilde{\Omega}_{\mathrm{PD}}(\sigma_2) \subseteq \tilde{\Omega}_{\mathrm{PD}}(\sigma_1)$.*
2) *For any index $\sigma_1 \succ 0$ s.t. $\Omega_{\mathrm{PD}}(\sigma_1) \neq \varnothing$, there exists a $\sigma_2 \succ \sigma_1$ s.t. $\Omega_{\mathrm{PD}}(\sigma_2) \subseteq \Omega_{\mathrm{PD}}(\sigma_1)$ if $|G(j\omega)| \neq 0$ holds for any $|\omega| < \infty$.*

Proof. The result $\Omega_{\mathrm{PD}}(\sigma) \subseteq \tilde{\Omega}_{\mathrm{PD}}(\sigma)$ directly comes from the necessity of Theorem 1. As for the contraction property, since $\sigma_2 \succ \sigma_1$, we have $\lambda_{\min}(\sigma_2) \geq \lambda_{\min}(\sigma_1)$. Theorem 1 suggests that if H meets the PD condition for σ_1, then we can always find a σ_2 s.t. $\Re(\rho_G(x)) > \lambda_{\min}(\sigma_2)|\rho_G(x)|^2 \geq \lambda_{\min}(\sigma_1)|\rho_G(x)|^2$ holds for arbitrary x satisfying $x^H x \neq 0$. Thus, H is also PD at frequency ω for σ_1. Therefore, any frequency in $\tilde{\Omega}_{\mathrm{PD}}(\sigma_2)$ must also be in $\tilde{\Omega}_{\mathrm{PD}}(\sigma_1)$, proving the first part of the contraction property.

For the second part of the contraction property, we consider the case $\Omega_{\mathrm{PD}}(\sigma_1) \neq [0, \infty]$ as otherwise it is trivial. Besides, we assume $\lambda_{\min}(\sigma) > 0$ and the case of $\lambda_{\min}(\sigma) < 0$ can be

derived similarly. Then, under these conditions, there exists a well-defined distance $d = \min_{\omega\in\Omega_{\rm PD}(\sigma_1)}(|G(j\omega)|)$, where $d \le 1/\sigma_1$ and $d > 0$ since $|G(j\omega)| \neq 0$. Take $1/(2\sigma_2) < d/2$, i.e., $\sigma_2 > 1/d$. Then, the distance of the new center $(1/(2\sigma_2), j0)$ to the Nyquist plot of $G(j\omega)$ is:

$$\left|G(j\omega) - \frac{1}{2\sigma_2}\right| \ge \left||G(j\omega) - 0| - (\frac{1}{2\sigma_2} - 0)\right| > d - \frac{d}{2} > \frac{1}{2\sigma_2} \tag{13}$$

Therefore, $\tilde{\Omega}_{\rm PD}(\sigma_2) = \varnothing$ and thus $\Omega_{\rm PD}(\sigma_2) = \varnothing \subseteq \Omega_{\rm PD}(\sigma_1)$. □

C. Dual Results for Input-Feedforward Passivization

The proposed method, obviously, also applies to visualizing the IF passivization. Moreover, due to the parallel structure of both G and σ, it is more trivial than the analysis of the OF counterparts. Consider the IF passivization $H = G - \sigma$. Then, the PD condition can be equivalently written as $G + G^H - 2\sigma \succeq 0$. Similarly, if employing the concept of the Rayleigh quotient, we obtain an estimated IF PD region as $\{\rho_G(x) : \rho_G(x) \ge \lambda_{\min}(\sigma), \forall x : x^H x \neq 0\}$. Following the ideas of OF passivization, we can visualize the PD region and derive the PD frequency band contraction property.

IV. Visualizing Passivization of SISO Systems

A. Positive Damping Condition

Theorem 2 (SISO PD Condition)**.** *Let $G(s)$ be a scalar transfer function satisfying Assumption 1. For a passivity index σ and a frequency $\omega \in \mathbb{R}$ where $j\omega$ is not a pole of G and $1 - \sigma G(j\omega) \neq 0$, the PD condition (1) is satisfied iff:*

$$\Re(G(j\omega)) \ge \sigma |G(j\omega)|^2 \tag{14}$$

Proof. Directly substitute $G(j\omega) = \Re(G(j\omega)) + j\Im(G(j\omega))$ into $H(j\omega) = G(j\omega)/(1 - \sigma G(j\omega))$, which yields:

$$\Re(H(j\omega)) = \left[\Re(G(j\omega)) - \sigma|G(j\omega)|^2\right] / |1 - \sigma G(j\omega)|^2 \tag{15}$$

Since the denominator is always positive, we have $H(j\omega) + H^H(j\omega) = 2\Re(H(j\omega)) \ge 0$ iff (14) holds, which completes the proof. □

B. Visualization of PD Region and Its Property

For SISO systems, the OF PD region satisfying the condition (14) in cases of $\sigma > 0$ can be equivalently rewritten as $\{G(j\omega) : G(j\omega) \in \mathcal{P}_{\rm PD}(\sigma)\}$, where:

$$\mathcal{P}_{\rm PD}(\sigma) = \mathcal{D}\left(\frac{1}{2\sigma} + j0, \frac{1}{2\sigma}\right) \tag{16}$$

This describes a disk in the complex plane, where $\partial\mathcal{D}$ centered at $(1/(2\sigma), j0)$ with radius $1/(2\sigma)$. The Nyquist plot of $G(j\omega)$ must lie within this disk for $H(j\omega)$ to meet the PD condition. The case of $\sigma < 0$ can be derived similarly.

Remark 2 (Relation with Möbius Transformation)**.** *For SISO systems, the geometric interpretation of OF passivization can be understood from another perspective. The definition (3) has defined a Möbius transformation from $G(s)$ to $H(s)$ w.r.t. σ, namely $H = G/(1 - \sigma G)$. When requiring the OF passivity of G w.r.t. σ, we desire that H meets the PD condition, i.e., always stays in the right half-plane. Consequently, it is equivalent to finding the pre-image G corresponding to the image of the right half-plane under the aforementioned Möbius transformation. Then, the result of Theorem 2 can also be derived from complex function theory. Furthermore, since IF passivization also implies a Möbius transformation $H = G - \sigma$, it can be visualized similarly.*

Moreover, this perspective suggests the proposed visualization also holds for discrete systems derived from the bilinear method. Consider Tustin's mapping $z = (1 + sT/2)/(1 - sT/2)$, which is also a Möbius transformation. Therefore, the circle-preservation property guarantees that the shape of the PD region will be preserved as a disk in the z-domain.

Similarly to MIMO systems, we can also derive the PD bandwidth contraction property for SISO systems. Due to the sufficiency of Theorem 2, the result is even stronger as shown below:

Corollary 3 (OF PD Bandwidth Contraction)**.** *Consider a scalar transfer function $G(s)$ satisfying Assumption 1. Then, $\tilde{\Omega}_{\rm PD}(\sigma) = \Omega_{\rm PD}(\sigma)$ holds that for its any passivity index σ. Besides, increasing σ contracts the PD frequency band, i.e., for any OF passivity indices σ_1 and σ_2 satisfying $\sigma_2 > \sigma_1$:*

$$\Omega_{\rm PD}(\sigma_2) \subseteq \Omega_{\rm PD}(\sigma_1) \tag{17}$$

Proof. We directly consider the scenarios where $\sigma_1 \neq 0$ and $\sigma_2 \neq 0$ since the otherwise scenarios are trivial. The result $\tilde{\Omega}_{\rm PD}(\sigma) = \Omega_{\rm PD}(\sigma)$ directly comes from the sufficiency and necessity of Theorem 2. The PD condition for SISO systems is $\Re(G(j\omega)) \ge \sigma|G(j\omega)|^2$. For a fixed ω, if this inequality holds for σ_2, then it automatically holds for σ_1 since $\sigma_1 < \sigma_2$. Therefore, any frequency in $\Omega_{\rm PD}(\sigma_2)$ must also be in $\Omega_{\rm PD}(\sigma_1)$, thus proving the contraction property. □

The derivation offers a depiction of the following intuition in Fig. 2: compared to classical passivity $\sigma = 0$, the OF passivization w.r.t. $\sigma > 0$ is more stringent. In contrast, $\sigma < 0$ allows certain systems that were previously non-passive to be rendered OF passive.

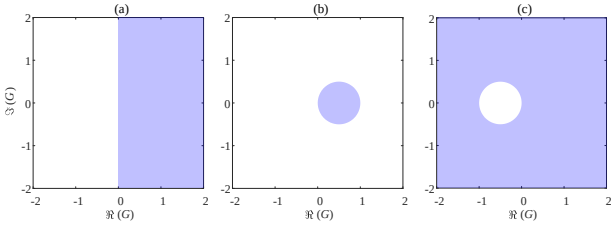

Fig. 2. Illustration of different PD regions $\mathcal{P}_{\rm PD}(\sigma)$ w.r.t. the passivity indices σ. (a): $\sigma = 0$, classical passivity definition. (b): σ =1. (c): σ =-1.

With the above interpretation, we can derive a geometric condition of OF passivization as follows:

Theorem 3 (Geometric OF Passivity Condition)**.** *Let $G(s)$ be a scalar rational transfer function satisfying Assumption 1 with no poles on the imaginary axis. Then, it is OF passive w.r.t. a passivity index $\sigma \neq 0$ if following conditions are satisfied:*

1) *The number of counter-clockwise revolutions made by the Nyquist plot of $G(s)$ around the point $(1/\sigma, j0)$ equals the number of unstable poles of $G(s)$.*
2) *The Nyquist plot of $G(s)$ does not go outside of the PD region $\mathcal{P}_{\mathrm{PD}}(\sigma)$.*
3) *The Nyquist plot of $G(s)$ does not intersect the point $(1/\sigma, j0)$.*

Proof. The conditions 1) and 3) can guarantee that H is stable following the proof of the well-known Nyquist criteria [3]. Therefore, the condition 1) of Definition 1 is satisfied. The condition 2) ensures the condition 2) of Definition 1 according to Theorem 2. Therefore, we focus on the correctness of the condition 3) of Theorem 2.

Since $G(s)$ is rational, $H(s)$ can be always written as

$$H(s) = \frac{N}{D - \sigma N} = \frac{n_0 + \sum_{i=1}^{n_n} n_i s^i}{\sum_{i=1}^{n_d}(d_i - \sigma n_i)s^i + d_0 - \sigma n_0} \tag{18}$$

where $N(s)$ and $D(s)$ are numerator and denominator of $G(s)$ and n_i and d_i are the coefficients of their i-th order terms, respectively. If existing pure imaginary poles for $H(s)$, it must be induced by $d_0 - \sigma n_0 = 0$ and the corresponding pure s on the denominator. However, as $G(0) = n_0/d_0 = 1/\sigma$ has been excluded by the condition 3), it is safe to guarantee the condition 3) of Definition 1, which completes the proof. □

If imaginary-axis poles exist, use the standard detour and the modified Nyquist criterion. Then, the same conclusions hold with the usual residue side conditions.

C. Robustness Analysis of Passivization

The geometric interpretation helps assess the robustness of passivization. Consider a nominal system $G_0(s)$. We then investigate the robustness of its OF passivity w.r.t. an index $\sigma > 0$. The analysis relies on the minimum distance of Nyquist plots to the boundary of PD regions defined as:

$$d_{\min}(\sigma) = \inf_{\omega \in \mathbb{R}} \left\{ \frac{1}{2\sigma} - \left| G_0(j\omega) - \frac{1}{2\sigma} \right| \right\} > 0 \tag{19}$$

When $G_0(s)$ is strictly OF passive, Theorem 2 guarantees $d_{\min} > 0$. Then, the robustness of OF passivization can be described as follows:

Theorem 4 (Robustness of Passivization)**.** *Let $G_0(s)$ be a nominal transfer function satisfying the conditions of Theorem 3. It is strictly OF passive w.r.t. a passivity index $\sigma > 0$ and has the distance defined in (19). Consider a perturbed system $G_p(s) = G_0(s) + \Delta(s)$ with the perturbation $\Delta(s)$ stable and its $\mathcal{H}_\infty$ norm denoted by $\|\Delta\|_\infty = \delta$. Then, $G_p(s)$ is also strictly OF passive w.r.t. the index σ if $\delta < d_{\min}$.*

Proof. Denote the PD region $\mathcal{P}_{\mathrm{PD}}(\sigma) = \mathcal{D}(c, r)$ with $c = r = 1/(2\sigma)$. Then, the PD condition follows directly from the triangle inequality $|G_p(j\omega) - c| = |G_0(j\omega) + \Delta - c| \le |G_0(j\omega) - c| + |\Delta| \le r - d_{\min} + \delta < r$. Thus, $G_p(j\omega)$ always stays in $\mathcal{D}(c, r)$. The other two conditions of strict passivity are trivial to verify by similar procedures as in Theorem 3. □

The robustness condition $\delta < d_{\min}$ has an intuitive geometric meaning: the maximum perturbation must be smaller than the minimum distance from the nominal Nyquist plot to the boundary of the PD region. This is a non-conservative condition if the perturbation is not subject to other constraints. In the sense that if $\delta > d_{\min}$, there exists a perturbation of that magnitude that could push the system outside the PD region at its most vulnerable frequency.

D. Integral Conservation of Passivization's Waterbed Effect

Theorem 2 suggests that the following $\varsigma(\omega)$ serves as a metric of OF passivizable ability at the frequency ω where $G(j\omega) \neq 0$:

$$\varsigma(\omega) = \frac{\Re(G(j\omega))}{|G(j\omega)|^2} = \Re\left(\frac{1}{G(j\omega)}\right) \tag{20}$$

The second equality can be derived through direct computation. A larger index $\varsigma(\omega)$ quantifies the system's stronger ability to be OF passivated and thus indicates a better damping effect at the frequency ω. It can be viewed as a generalized OF passivity index defined frequency-wise and satisfies $\sigma \le \varsigma(\omega)$ as delineated in (14). However, we show $\varsigma(\omega)$ cannot be strengthened at all frequencies for a specific system but follows a conservation law, akin to the *waterbed effect* [13].

Specifically, we consider a strictly proper rational and minimal-phase LTI system $G(s)$. Then, it can be reformulated as $1/G(s) = L(s) + C + R(s)$, where $L(s)$, C, and $R(s)$ are the polynomials without the constant term, constant terms, and strict rational functions, respectively. The order of $L(s)$ equals the relative degree n_r of $G(s)$. Decompose $f(s) = 1/G(s) - L(s) = C + R(s)$. Then the minimal-phase assumption guarantees that $f(s)$ is analytic on the closed right-half plane and satisfies $\lim_{D\to\infty} \sup_\theta |f(De^{j\theta})|/D = 0$. Therefore, $\Re(f(s))$ is harmonic on the same region and follows the Poisson formula [13, Appendix A]:

$$\pi \Re(f(a)) = \int_{-\infty}^{\infty} \Re(f(j\omega)) \mathscr{P}_a(\omega) \mathrm{d}\omega \tag{21}$$

where $a \in \mathbb{R}$ is not any poles of $R(s)$ and $\mathscr{P}_a(\omega) = a/(\omega^2 + a^2)$ is called the Poisson kernel. The constant a regulates the shapes of the kernel, and a smaller a indicates more concern for the low-frequency bands. For a given system, a should be predetermined as a constant. Substituting the definition of $f(s)$ yields:

$$\frac{1}{G(a)} - L(a) = \frac{1}{\pi} \int_{-\infty}^{\infty} [\varsigma(\omega) - \Re(L(j\omega))] \mathscr{P}_a(\omega) \mathrm{d}\omega \tag{22}$$

Consider the systems with relative degree $n_r = 1$ as an example, which includes various practical dynamics. For higher relative degrees $n_r > 1$, one obtains additional polynomial subtraction terms in the right-hand side of (22), but the qualitative conservation persists. For $n_r = 1$, we can write $L(s) = l_1 s$ where $l_1 = 1/(\lim_{s\to\infty} sG(s))$ is a real coefficient and (22) reduces to:

$$\frac{1}{G(a)} - l_1 a = \frac{1}{\pi} \int_{-\infty}^{\infty} \varsigma(\omega) \mathscr{P}_a(\omega) \mathrm{d}\omega \tag{23}$$

which implies that the (Poisson-weighted) integral of $\varsigma(\omega)$ over the entire frequency bands is conservative for a given system $G(s)$. Therefore, increased damping in some bands (larger

ς) will force reductions elsewhere. For instance, suppose we hope $\varsigma(\omega) \geq \sigma$ for $|\omega| \leq \omega_c$ and $\varsigma(\omega) \geq 0$ for $|\omega| > \omega_c$. Then, (23) with $a > 0$ yields:

$$\frac{1}{G(a)} - l_1 a \geq \frac{1}{\pi}\int_{-\omega_c}^{\omega_c} \varsigma(\omega)\mathscr{P}_a(\omega)\mathrm{d}\omega \geq \frac{\sigma}{\pi}\int_{-\omega_c}^{\omega_c} \mathscr{P}_a(\omega)\mathrm{d}\omega \tag{24}$$

Direct computation leads to $1/G(a) - l_1 a \geq \sigma/\pi \arctan(\omega_c/a)$. This inequality clearly shows that the passivizable frequency bandwidth ω_c and the passivity index σ cannot be simultaneously extended for a predetermined transfer function $G(s)$.

V. Extension to Generalized Definition

Definition 6 ($\mathcal{R}$-Output-Feedback Passivization)**.** *A $p \times p$ LTI system $G(s)$ is $\mathcal{R}$-OF passivizable w.r.t. a symmetric matrix $\sigma \in \mathbb{R}^{p\times p}$ and a rational bounded operator $\mathcal{R}$ if $H^D(s)$ defined in (25) is passive:*

$$H^D(s) = \mathcal{R}(s) \cdot (I - G(s)\sigma)^{-1}G(s) \tag{25}$$

The matrix σ is called its $\mathcal{R}$-OF passivity index.

The operator $\mathcal{R}$ generalized several existing passivity definitions and reduces to the classical one by letting $\mathcal{R} = I$. Some extensions employed in power system analysis are:

Example 1. *Let $\mathcal{R} = s$ as the differential passivity [2], also recognized as negative imaginariness [11]. Then, the condition (26) is equivalent to $\Im(G) \leq 0$ for $\forall\omega \geq 0$, which corresponds to the lower half plane.*

Example 2. *Let $\mathcal{R} = 1$ and $sG(s)$ replacing $G(s)$ [14]. Then, the condition (26) is equivalent to $\omega\sigma|G|^2 + \Im(G) \leq 0$ for $\forall\omega \geq 0$, When $\sigma > 0$, it represents a disk with $\partial\mathcal{D}$ centered on the imaginary axis.*

Theorem 5 (SISO PD Condition for Generalized Definition)**.** *Let $G(s)$ be a scalar transfer function satisfying Assumption 1. For a passivity index σ and a frequency ω with $j\omega$ not a pole of G or $\mathcal{R}$ and $1 - \sigma G(j\omega) \neq 0$, the PD condition (1) is satisfied at the frequency ω iff:*

$$\begin{aligned}\Re(\mathcal{R}(j\omega))\Re(G(j\omega)) - \Im(\mathcal{R}(j\omega))\Im(G(j\omega)) \\ \geq \sigma|G(j\omega)|^2\Re(\mathcal{R}(j\omega))\end{aligned} \tag{26}$$

Proof. Substitute $\mathcal{R}(j\omega) = \Re(\mathcal{R}(j\omega)) + \Im(\mathcal{R}(j\omega))$ into (25) and then the following procedures are similar to the proof of Theorem 2. □

To deal with possibly existing explicit ω in $\mathcal{R}(j\omega)$, consider a 3-dimension coordinate $(\Re(G(j\omega)), \Im(G(j\omega)), \omega)$. Similarly, the region where $(\Re(G(j\omega)), \Im(G(j\omega)), \omega)$ satisfies the condition (26) is denoted as its *PD region*. Then, it is easy to derive the following results regarding the PD frequency band:

Corollary 4. *Consider a scalar transfer function $G(s)$ satisfying Assumption 1 w.r.t. a passivity index σ and define its PD frequency bands $\Omega^D_{\mathrm{PD}}(\sigma) = \{\omega \geq 0 : H^D(j\omega) + (H^D)^H(j\omega) \succeq 0\}$. Then, $\Omega^D_{\mathrm{PD}}(\sigma) = \{\omega \geq 0$: the condition (26) is satisfied.$\}$*

VI. Encoding Passivization into Classic Tools

The method's simplicity allows it to be encoded into various classic analysis and design tools. In various applications, the configuration illustrated in Fig. 1 comprises an uncontrollable G_2 and a controllable G_1. In these instances, the OF passivity index σ for G_1 is commonly predetermined or has a minimum threshold to guarantee the closed-loop stability.

As an example, in the distributed stability analysis of power systems [2], G_2 represents the power network with an IF passivity index $\sigma_2 < 0$, which, however, is usually challenging to regulate. The proposed method then suggests that, to maintain closed-loop stability, it suffices for the device dynamics G_1 to fall within the PD region w.r.t. $\sigma_1 > -\sigma_2$. Importantly, it is not required for G_1 to adhere to a specific structural framework or even to possess an analytical formulation. By alleviating the model requirements, the proposed method enhances the flexibility of device control designs.

A. Graphic Analysis on Nyquist and Nichols Plots

The above analysis presents the proposed condition in Nyquist plots using the $\Re(G) - \Im(G)$ coordinates. Apart from that, it is also easily applicable to the Nichols plot with $\log|G| - \angle G$ coordinates. Specifically, (14) can be equivalently transformed as $20\log|G(j\omega)| \leq 20\log|\cos(\angle G)| - 20\log(\sigma)$, which holds for any ω satisfying $|\angle G(j\omega)| \leq \pi/2$. The Nichols plot intuitively displays the system's dynamic performance, such as gain margin, phase margin, resonant peak, and bandwidth under unit negative feedback. Thus, it holds significance in applications such as circuit and aircraft controls [15]. An example of the Nichols plot is shown in Fig. 3.

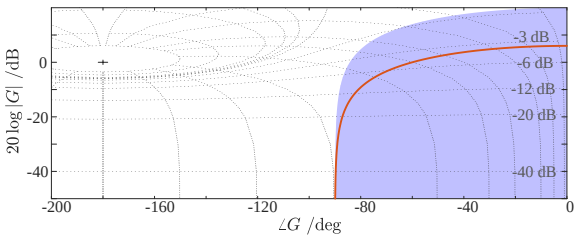

Fig. 3. Nichols plot with the PD region. The orange curve is the Nyquist plot of G_1 with expressions provided in (28), and the PD region $\mathcal{P}_{\mathrm{PD}}(0.1)$ is represented by the purple region.

Utilizing the Nichols plot, control designs can be performed by deploying the classic frequency-response shaping method. The proposed method does not alter the fundamental approach of frequency response shaping; rather, it introduces an additional performance requirement wherein the trajectory must stay within the PD region (e.g., the purple region in Fig. 3), thereby ensuring that G_1 is OF passive w.r.t. the index σ_1. Therefore, we refer interested readers to [15, Chapter 9] for further details on the specific design and tuning procedures.

B. Generalized-KYP-Based Parameter Tuning

The proposed PD region can be transformed into LMI constraints by employing the generalized KYP lemma [9]. This lemma guarantees that if the Nyquist plot of some

widely-used transfer function lies within a specific hyperbolic region over a given frequency band, it possesses an equivalent LMI formulation. Thereby, the control design problem can be transformed into convex feasibility or optimization problems. Similarly, we emphasize that the proposed method does not alter the fundamental workflow of control design based on the generalized KYP lemma. In contrast, it merely introduces an additional constraint. Moreover, the PD region is a disk in the complex plane and can thus be expressed as LMI constraints.

Specifically, consider a plant $P(s)$ with the minimal realization (A, B, C, D) and a (proportional-integral-differential) PID controller $K(s) = k_p + k_i/s + k_d s/(\tau s + 1)$, where τ is a given filter time constant. It is desired that $G = PK$ is OF passive over the frequency bands $|\omega| \le \omega_c$ w.r.t. an index $\sigma > 0$. First, the PD condition $G(j\omega) \in \mathcal{D}(1/(2\sigma), 1/(2\sigma))$ can be equivalently expressed as:

$$\begin{bmatrix} G(j\omega)^H & 1 \end{bmatrix} \begin{bmatrix} 1 & -1/(2\sigma) \\ -1/(2\sigma) & 1 \end{bmatrix} \begin{bmatrix} G(j\omega) \\ 1 \end{bmatrix} \le 0 \quad (27)$$

Then, by directly using [16, Proposition 1], the desired results achieves if the LMI $\mathcal{W}(P, Q, A, B, C, D, k_p, k_i, k_d) \preceq 0$ exists Hermitian solution matrices P and $Q \succeq 0$. The specific expression of $\mathcal{W}$ can be found in [16, Proposition 1].

Here, the dynamics of PID controllers serve as an example of $G(s)$, and the method is extendable. By encoding this constraint, along with other performance constraints, automatic tuning of control parameters can be performed while rendering the system OF passive. For the interested reader, we refer to [16] for details on its applications in control design.

VII. Application to Visualized Passivity Analysis

For illustration, this section employs the following transfer functions in (28), which are derived from electrical power system stability analysis and control system design. Here, G_1, G_2, G_3 and G_4 represent the voltage regulation dynamics [2], phase-angle dynamics [2], frequency swing dynamics with power filter [2], and angle-voltage coupled control strategy with cross-loop control gain $G_c = C/(Ts + 1)$ [17], respectively. In the simulation, we use the following parameters: $\tau = 0.1$, $k = 0.5$, $M = 0.3$, $d = 0.5$, $T = 0.02$, and $C = 0.1$.

$$\begin{aligned} G_1 &= \frac{1}{\tau s + k} & G_2 &= \frac{1}{s(Ms + d)} \\ G_3 &= \frac{1}{(Ts + 1)(Ms + d)} & G_4 &= \begin{bmatrix} G_3 & G_c \\ G_c & G_1 \end{bmatrix} \end{aligned} \quad (28)$$

All figures and numerical results in this paper can be reproduced using the data and code available at https://github.com/lingo01/Geometric_Passivization.

A. Graphic Analysis of Classical Passivity

The PD region $\mathcal{P}_{\mathrm{PD}}(1)$ is indicated by the red disk in Fig. 4(a). Since the Nyquist plot of the open-loop transfer function G_1 is outside this region at all frequencies, G_1 cannot be OF passivized throughout the frequency bands w.r.t. the index $\sigma = 1$. To ensure that $G_1(j\omega) \in \mathcal{P}_{\mathrm{PD}}(\sigma)$ for all ω, the diameter of the disk $1/\sigma$ must be greater than the rightmost point of the Nyquist plot, which is $1/k = 2$. Here, we select $1/\sigma = 3$, corresponding to the purple disk, under which G_1 becomes OF passivizable w.r.t. the passivity index $\sigma = 1/3$.

Fig. 4(b) shows the Nyquist plot of G_2 cannot intersect any disk w.r.t. $\sigma \ge 0$, implying that G_2 cannot be passivized via OF for any positive $\sigma \ge 0$. Although this conclusion can be derived analytically, the proposed geometric approach offers a more intuitive interpretation.

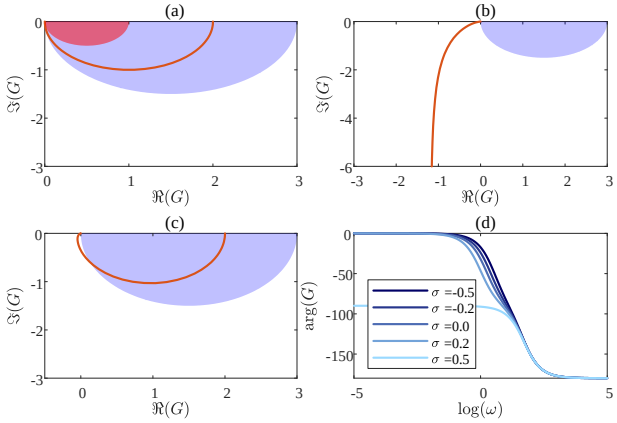

Fig. 4. Application to SISO systems. (a): Nyquist plot (orange curve) of G_1 and the PD region $\mathcal{P}_{\mathrm{PD}}(1)$ (purple disk) and $\mathcal{P}_{\mathrm{PD}}(1/3)$ (red disk). (b): Nyquist plot of G_2 and the PD region $\mathcal{P}_{\mathrm{PD}}(1/3)$. (c): Nyquist plot of G_3 and the PD region $\mathcal{P}_{\mathrm{PD}}(1/3)$. (d): phase-angle part of the Bode plot of G_3.

The Nyquist plot of G_3 is shown in Fig. 4(c). It can be visually confirmed that G_3 cannot be fully passivized across all frequencies, especially the high-frequency bands. For the purple disk w.r.t. $\sigma = 1/3$, the system meets the PD condition only when the Nyquist curve lies inside the disk, corresponding to the critical frequency $\omega_c \le 5.3703$. Moreover, as σ increases, the PD frequency band monotonically contracts as analyzed in previous sections. As illustrated in Fig. 4(d), for σ = -0.5, -0.2, 0, 0.2, 0.5, the critical frequencies are 13.1826, 10.9648, 9.3325, 7.0795, and 0.0000, respectively.

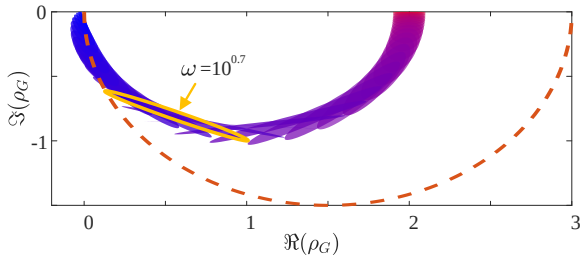

Fig. 5. Application to MIMO systems. The orange dashed circle denotes the PD region $\mathcal{P}_{\mathrm{PD}}(1/3 \cdot I)$. Each colored disk represents the Rayleigh quotient $\rho_G(j\omega)$ at a given frequency ω. For example, the yellow circle represents the boundary of all possible values of the Rayleigh quotient $\rho_{G(j10^{0.7})}(x)$, which intersects the PD region. Here we present the frequencies which $\log(\omega)$ from -3 to 2 with a sampling interval of 0.1.

The analogous analysis remains applicable to MIMO systems. Fig. 5 illustrates the Rayleigh quotient as delineated in $G_4(j\omega)$ and the PD region w.r.t. the passivity index $\sigma = 1/3 \cdot I$. According to Theorem 1, G_4 cannot satisfy the PD condition (1) and thus cannot be OF passivized in the frequency band $\omega \ge 10^{0.7}$, where the Rayleigh quotient cannot consistently reside within the PD region.

B. Graphic Analysis of Generalized Passivity

Fig. 6 illustrates the PD regions of G_2 and G_3 under the definition of differential passivity (or negative imaginariness) in Example 1. It can be observed that for any negative imaginary transfer function, the differential passivity meets the PD condition for the OF system, which also explains its advantageous applicability in power systems [2]. However, it should be noted that this does not imply that an arbitrary σ can render the transfer function passive. This is because, in addition to the PD condition, passivity must also satisfy conditions 1) and 3) in Definition 1, which can be guaranteed geometrically in a similar approach to Theorem 3. For G_2, to ensure that its Nyquist plot, as shown in Fig. 6(a), does not encircle the point $(1/\sigma, j0)$, it is necessary to choose $1/\sigma < 0$. For G_3, to prevent its Nyquist plot in Fig. 6(b) from encircling the point $(1/\sigma, j0)$, the condition $1/\sigma > 1/d$ must be satisfied, i.e., $\sigma < d$, which aligns with [2], [14].

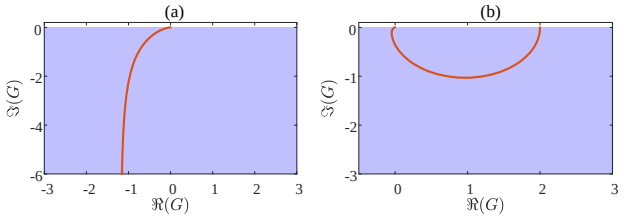

Fig. 6. Application to differential passivization in Example 1. (a): Nyquist plot (orange curve) of G_2 with PD region (purple square). (b): Nyquist plot of G_3 with the PD region.

The PD region for the generalized passivity in Example 2 is presented in Fig. 7. The case for $\sigma = 0.1$ is shown in Fig. 7(a). The Nyquist plots of all three transfer functions G_1, G_2, and G_3 lie entirely within the PD region, indicating that the corresponding systems are OF passivizable. Furthermore, we examine the cases for different values of σ. The corresponding PD regions for $\sigma = 0.1$, 0.3, and 1.0 are displayed in Fig. 7(b). Firstly, it can be observed that the region contracts as σ increases. Secondly, for G_2, it has a positive damping only for $\sigma = 0.1$ and 0.3, while certain frequency bands fall outside the region w.r.t. $\sigma = 1.0$ and thus are non-passivizable.

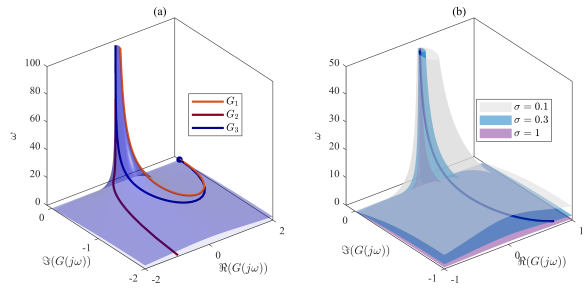

Fig. 7. Application to Example 2 passivization. (a): PD region w.r.t. σ =0.1 (purple region) and the Nyquist plots of G_1, G_2, and G_3. (b): PD regions w.r.t. σ =0.1, 0.5 and 1.0 and the Nyquist plot of G_3.

VIII. Conclusion

This work establishes a geometric framework for passivization analysis. By demonstrating that IF and OF passivizations are equivalent to the Nyquist plot or Rayleigh quotient lying within a specific region depending on the passivity index, we transform the analysis into an intuitive visual inspection. Furthermore, the proposed method can be integrated into classical geometric analysis and design tools, such as the Nichols plot and generalized-KYP-lemma-based controller design methods.

This geometric perspective not only elucidates fundamental trade-offs, such as the contraction of the positive damping bandwidth with increasing passivity index, but also provides a unified platform for analyzing both classical and generalized passivity definitions. The efficacy of this approach is validated through illustrative examples from power systems, highlighting its potential to simplify and guide stability analysis and control design. Future work will focus on generalizing this visualization method to nonlinear systems and leveraging it for the synthesis of practical inverter controllers.

References

[1] N. Kottenstette, M. J. McCourt, M. Xia, V. Gupta, and P. J. Antsaklis, "On relationships among passivity, positive realness, and dissipativity in linear systems," *Automatica*, vol. 50, no. 4, pp. 1003–1016, 2014.

[2] P. Yang, F. Liu, Z. Wang, and C. Shen, "Distributed stability conditions for power systems with heterogeneous nonlinear bus dynamics," *IEEE Transactions on Power Systems*, vol. 35, no. 3, pp. 2313–2324, 2020.

[3] K. Hassan, *Nonlinear Systems*. Prentice Hall, 1996.

[4] F. Chen, S. Z. Khong, X. Wang, and L. Harnefors, "Unified and Flexible Frequency-Domain Stability Assessment Framework for Power-Electronic-Based Power Systems," *IEEE Transactions on Power Electronics*, pp. 1–6, 2025.

[5] L. Huang, D. Wang, X. Wang, H. Xin, P. Ju, K. H. Johansson, and F. Dörfler, "Gain and Phase: Decentralized Stability Conditions for Power Electronics-Dominated Power Systems," *IEEE Transactions on Power Systems*, vol. 39, no. 6, pp. 7240–7256, 2024.

[6] S. Z. Khong and A. Lanzon, "Feedback Stability Analysis via Frequency Dependent Constraints," *IEEE Transactions on Automatic Control*, vol. 70, no. 2, pp. 1228–1235, 2025.

[7] D. de S. Madeira, "Necessary and Sufficient Dissipativity-Based Conditions for Feedback Stabilization," *IEEE Transactions on Automatic Control*, vol. 67, no. 4, pp. 2100–2107, 2022.

[8] S. Grivet-Talocia, "Passivity enforcement via perturbation of Hamiltonian matrices," *IEEE Transactions on Circuits and Systems I: Regular Papers*, vol. 51, no. 9, pp. 1755–1769, 2004.

[9] T. Iwasaki and S. Hara, "Generalized KYP lemma: Unified frequency domain inequalities with design applications," *IEEE Transactions on Automatic Control*, vol. 50, no. 1, pp. 41–59, 2005.

[10] P. Seiler, A. Packard, and P. Gahinet, "An Introduction to Disk Margins," *IEEE Control Systems Magazine*, vol. 40, no. 5, pp. 78–95, 2020.

[11] J. Xiong, I. R. Petersen, and A. Lanzon, "A negative imaginary lemma and the stability of interconnections of linear negative imaginary systems," *IEEE Transactions on Automatic Control*, vol. 55, no. 10, pp. 2342–2347, 2010.

[12] W. Chen, D. Wang, S. Z. Khong, and L. Qiu, "A phase theory of multi-input multi-output linear time-invariant systems," *SIAM Journal on Control and Optimization*, vol. 62, no. 2, pp. 1235–1260, 2024.

[13] M. M. Seron, J. H. Braslavsky, and G. C. Goodwin, *Fundamental Limitations in Filtering and Control*, ser. Communications and Control Engineering. London: Springer London, 1997.

[14] X. Peng, C. Fu, Z. Li, X. Ru, Z. Wang, and F. Liu, "Compositional grid codes with guarantee on both stability and dynamic performance," *IEEE Transactions on Power Systems*, 2026.

[15] R. Dorf and R. Bishop, *Modern Control Systems, Global Edition*. Harlow: Pearson Education Limited, 2022.

[16] S. Hara, T. Iwasaki, and D. Shiokata, "Robust PID control using generalized KYP synthesis: Direct open-loop shaping in multiple frequency ranges," *IEEE Control Systems Magazine*, vol. 26, no. 1, pp. 80–91, 2006.

[17] X. Peng, C. Fu, P. Yang, X. Ru, and F. Liu, "Impact of angle-voltage coupling on small-signal stability of power systems: A damping perspective," *IEEE Transactions on Circuits and Systems I: Regular Papers*, 2025.